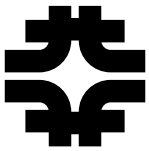

Fermi National Accelerator Laboratory

FERMILAB-Pub-95/310-E
CDF

CDF Results on Top

Andrew Beretvas
For the CDF Collaboration

Fermi National Accelerator Laboratory
P.O. Box 500, Batavia, Illinois 60510

September 1995

Submitted to *International Journal of Modern Physics A*

Operated by Universities Research Association Inc. under Contract No. DE-AC02-76CHO3000 with the United States Department of Energy

Disclaimer

This report was prepared as an account of work sponsored by an agency of the United States Government. Neither the United States Government nor any agency thereof, nor any of their employees, makes any warranty, expressed or implied, or assumes any legal liability or responsibility for the accuracy, completeness, or usefulness of any information, apparatus, product, or process disclosed, or represents that its use would not infringe privately owned rights. Reference herein to any specific commercial product, process, or service by trade name, trademark, manufacturer, or otherwise, does not necessarily constitute or imply its endorsement, recommendation, or favoring by the United States Government or any agency thereof. The views and opinions of authors expressed herein do not necessarily state or reflect those of the United States Government or any agency thereof.

International Journal of Modern Physics A,
© World Scientific Publishing Company

CDF/TOP/PUBLIC/3317
Version 2.0
September 20, 1995

CDF Results on Top

Andrew Beretvas
for the CDF Collaboration
Fermi National Accelerator Laboratory
Batavia Illinois 60510, USA

Received (received date)
Revised (revised date)

CDF has established the existence of the top quark. Results from $p\bar{p}$ collisions at $\sqrt{s}$ = 1.8 TeV are presented. In the dilepton final state we find seven events with a background of 1.3 ± 0.3. In the e, $\mu + \nu$ + jets channel with a b identified via a secondary vertex detector (SVX), we find twenty one events with a background of 5.5 ± 1.8. We measure the top quark mass to be 176 ± 8 (stat) ± 10 (syst) GeV/c^2, and the $t\bar{t}$ production cross section to be $7.6^{+2.4}_{-2.0}$pb. The integrated luminosity for the results presented in this talk is 67 pb^{-1}. The CDF detector needs to be upgraded for our next run. The integrated luminosity for the next run is expected to be more than 1000 pb^{-1}.

1. Introduction

This paper, presented at the International Symposium on Particle Theory and Phenomenology on May 22, is about the CDF observation of top. [1] The topics covered will be the dilepton analysis, a few words about the detector, doing b-physics with the silicon vertex detector, the SVX b-tag analysis, the cross section and the mass analysis. The CDF Collaboration consists of 440 physicists (Fig. 1).

We have been doing collider physics for a long time. Collisions were detected in 1985. Our first Physics run with an integrated luminosity of 25 nb^{-1} took place in 1987-88. Our next run (1988-89) with a luminosity of 4 pb^{-1} resulted in a limit on the top mass of greater than 91 GeV/c^2. [2] This limit was primarily determined from the number of dilepton events. In Run 1a (1992-93, luminosity = 19.3 pb^{-1}) we presented evidence for the existence of the top quark. [3] This evidence depends on the observation of dilepton events, and lepton plus 3 or more jets, where one of the jets is tagged as a b jet. The b jet is tagged using either SVX tracking information to find a displaced vertex or a soft lepton tag (SLT) indicating a b decay (b → l ν X, or b → c → l ν X). In fall 1994 we reported additional evidence for a top component in our W + jet sample from a study of the transverse energy of the leading jets. [4] Earlier this year we reported the observation of the top quark. [1] This observation is also based on the dilepton and b-tag (SVX and SLT) modes but with better statistics. This paper refers to the same sample as reported in Ref. 1 with a

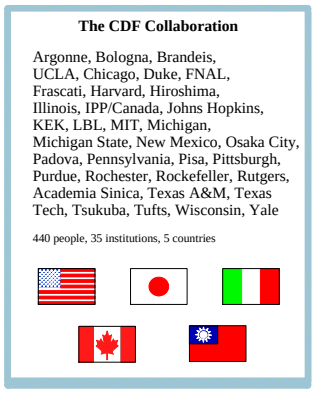

Figure 1: The CDF collaboration consists of 440 physicists at 35 institutions in 5 countries.

combined luminosity from run 1a and 1b of 67 pb^{-1} (note that as of June 12, 1995 the combined luminosity was over 100 pb^{-1}).

The Tevatron collider luminosity has increased with each run. The reader interested in the status of the Tevatron should read Ref. 5. The design luminosity for the Tevatron was 10^{30} $cm^{-2}s^{-1}$. Today the typical luminosity is between 1.4 and 2.0×10^{31} $cm^{-2}s^{-1}$. The standard expression for the luminosity is given in Fig. 2. In the formula ϵ is the emittance. Some typical values for run 1a are given in Fig. 3.

For run 1b we have typical values of $N_p = 22.5 \times 10^{10}$ protons/bunch, $N_{\overline{p}} = 6.5 \times 10^{10}$ antiprotons/bunch, the number of bunches is 6, the typical value for the form factor (F) is 0.62, the proton (antiproton) emittance is 22 (14) π mm-mrad and the value of $\beta^\star$ at the interaction point is 35 cm. Note these typical values yield a luminosity of $1.9 \times 10^{31} cm^{-2}s^{-1}$.

The ultimate phase space density is limited by the beam-beam tune shift which at the present operating point is 1.5×10^{10} particles per π mm-mrad. During run 1b the single bunch proton (antiproton) phase space density is 1.0 (0.6) $\times$ 10^{10} particles per π mm-mrad. This indicates that to increase the luminosity we need to increase the number of bunches. After the main injector is completed in 1998, we will start run 2 in early 1999. For this run we will have 36 bunch operation resulting in a typical luminosity of 2.0×10^{32} $cm^{-2}s^{-1}$. These estimates may be low and luminosity a factor of 5 higher may be possible. [6]

As recalled, it has taken a long time for us to observe the top quark. The reason for this is obvious, namely the low cross section for $t\bar{t}$ production. The search for top has been CDF's top priority for many years. But clearly we also have done much other physics. At the present time we are writing out data at the rate of 6 Hz, where each event is approximately 100 Kbytes. As of April-1995 we had written out over 30 M events. The top analysis is done from an express line. The number of events in the express line is about 2 M, which corresponds to 2×10^{11} bytes.

The fact that we have finally been able to observe the top quark is due to the

high luminosity achieved by the accelerator. The $p\bar{p}$ total cross section (80.03 ± 2.24 mb) is more than 10^{10} larger than the top cross section ($6.8^{+3.6}_{-2.4}$ pb). [1] For the dilepton mode there is an additional reduction factor of 100. Indeed, only about 5% of the $t\bar{t}$ decay via the dilepton mode, and of these we are only able to detect about 1 in 5.

Accelerator Parameters

$$L = N_B f_0 \frac{N_p N_{\bar{p}}}{4\pi\sigma_V\sigma_H} F$$

- N_B Number of Bunches
- f_0 Revolution frequency
- N_p Protons/Bunch
- $N_{\bar{p}}$ Anti-Protons/Bunch
- F Form Factor

$$\sigma_V^2 = \left(\frac{\epsilon_p^V + \epsilon_{\bar{p}}^V}{2}\right)\frac{\beta_V^\star}{6\pi\beta\gamma}$$

$$\sigma_H^2 = \left(\frac{\epsilon_p^H + \epsilon_{\bar{p}}^H}{2}\right)\frac{\beta_H^\star}{6\pi\beta\gamma}$$

Figure 2: Expression for the luminosity.

Typical Luminosity for run 1a
$\mathcal{L} = 5.4 \times 10^{30}\mathrm{cm}^{-2}\mathrm{s}^{-1}$

- $N_B = 6$
- $f_0 = 4.8 \times 10^4$ s^{-1}
- $N_p = 1.2 \times 10^{11}$
- $N_{\bar{p}} = 3.6 \times 10^{10}$
- F = 0.76
- $\epsilon = 16\pi$ mm-mrad $= 16\pi \times 10^{-4}$cm
- $\beta^\star = 50$ cm
- $\beta\gamma$ = p/m = 9.6×10^2
- $\sigma^2 = 1.4 \times 10^{-5}$ cm^2

run 1b $\mathcal{L} = 1.4 \times 10^{31}\mathrm{cm}^{-2}\mathrm{s}^{-1}$

- $N_B = 36$

run 2 $\mathcal{L} = 8.3 \times 10^{31}\mathrm{cm}^{-2}\mathrm{s}^{-1}$

Figure 3: The numbers are presented for a typical luminosity calculation for run 1b. We expect to maintain the present number of protons in each bunch as we go to 36 bunch operation in Run 2. Even more optimistic estimates exist for Run 2 (10^{33} cm^{-2}s^{-1}.)

2. Dilepton Analysis

The branching ratio for the three decay modes of the top are 44% for the hadronic, 44% for the lepton plus jet, and only 11% for the dilepton (Fig. 4). Although we are making progress on looking at the all hadronic mode, this paper will refer to only the lepton plus jet and dilepton modes. At this time we will report only on modes involving an electron or a muon. Thus the relevant branching fractions are 29.6% for the lepton plus jet and 4.9% for the dilepton modes. We look at the dilepton mode by requiring two oppositely charged high P_T leptons and a neutrino (large $\not\!\!E_T$).

The numerical values of the dilepton detection efficiencies are given in table 1. A

P_T threshold of 20 GeV for each lepton is chosen to preserve a large portion of the top signal and to suppress the backgrounds. For central electrons at pseudorapidity $| \eta | < 1$. we apply several cuts to eliminate hadrons. These include a cut on the ratio of the hadronic to electromagnetic energy of the cluster (HAD/EM), the ratio of the cluster energy to track momentum (E/P), a comparison of the lateral shower profile (L_{sh}) in the calorimeter cluster with that of test beam electrons, the distance between the extrapolated track position and strip chamber shower position measured in the ϕ and z views, and a χ^2 comparison of the strip chamber shower profiles with those of test beam electrons. In general one lepton requires a tight cut and the other a loose cut. At least one central lepton in each event must pass a track isolation cut $I_{track} < 3$ GeV/c where I_{track} is the sum of the P_T over all tracks in a cone of radius 0.25 (in $\eta - \phi$ space) centered on the lepton track. The trigger requirements are very efficient as one has two chances to pass a single high P_T lepton trigger. For details that also include plug electron and muons, see Ref. 3. Conversions and same sign dileptons are also removed. There are 3 topology cuts. The first eliminates backgrounds from Z decays, by cutting on the dilepton invariant mass. The second cut requires $\not\!\!E_T > 25$ GeV and removes backgrounds from $Z \rightarrow \tau\tau$, $b\bar{b}$ and lepton misidentification. For events with $\not\!\!E_T < 50$ GeV, the third cut requires that $\Delta\phi(\not\!\!E_T, \text{lepton}) > 20°$ and $\Delta\phi(\not\!\!E_T, \text{jet}) > 20°$, where $\Delta\phi(\not\!\!E_T, \text{lepton or jet})$ is the azimuthal angle between the $\not\!\!E_T$ and the direction of the nearest lepton or jet. Finally we require two jets with $\eta < 2.0$ to have uncorrected transverse energy greater than 10 GeV. The results of all these cuts is a dilepton detection efficiency of 17.3 ± 1.5 %.

Table 1. Dilepton detection efficiency

Cuts	efficiency(%)
GEOM P_T	0.74
Lepton identification	0.43
Lepton Isolation	0.96
Trigger	0.97
Topology	0.66
Two-Jet	0.88
Total	0.17

From the 2M express line events, the number of high P_T isolated lepton events is about 48K electrons and 32 K muons. The number of events as a function of cuts is given in table 2. After all the cuts there are no ee events, two $\mu\mu$ events, and five eμ events. The distribution of these events in a scatter plot of $\Delta\phi$ versus $\not\!\!E_T$ is given in Figs. 5, 6, and 7. The scatter plot shows how clean the plots become after the 2 jet requirement.

Five different physics processes are considered as contributing to the dilepton background. These are Drell-Yan, $p\bar{p} \rightarrow Z \rightarrow \tau\tau$, fake leptons, $p\bar{p} \rightarrow WW$, and $p\bar{p} \rightarrow b\bar{b}$. The total background is 1.3 ± 0.3 events. To be conservative in estimating a

• Decay Modes for a $t\bar{t} \rightarrow W^+bW^-\bar{b}$

Decay Mode	Branching ratio
All Hadronic	36/81 = 44.4%
6 Jets qqb qq$\bar{b}$	
Lepton + Jets	36/81 = 44.4%
qqb e$\nu\bar{b}$	12/81 = 14.8%
qqb $\mu\nu\bar{b}$	12/81 = 14.8%
qqb $\tau\nu\bar{b}$	12/81 = 14.8%
Lepton + 4 Jets	29.6%
Dilepton	9/81 = 11.1%
eνb $\mu\nu\bar{b}$	2/81 = 2.5%
eνb $\tau\nu\bar{b}$	2/81 = 2.5%
$\mu\nu$b $\tau\nu\bar{b}$	2/81 = 2.5%
eνb e$\nu\bar{b}$	1/81 = 1.2%
$\mu\nu$b $\mu\nu\bar{b}$	1/81 = 1.2%
$\tau\nu$b $\tau\nu\bar{b}$	1/81 = 1.2%
Dilepton + 2 Jets	4.9%

Figure 4: The standard model branching fractions are given for $t\bar{t}$ decay.

Table 2. Dilepton data for 67 pb^{-1}

	ee	$\mu\mu$	$e\mu$
Lepton ID	2146	2220	39
Same Sign	2118	2211	29
Isolation	2079	2148	25
Z Mass	215	233	25
Missing E_T	5	4	9
2-jet (10 GeV)	0	2	5

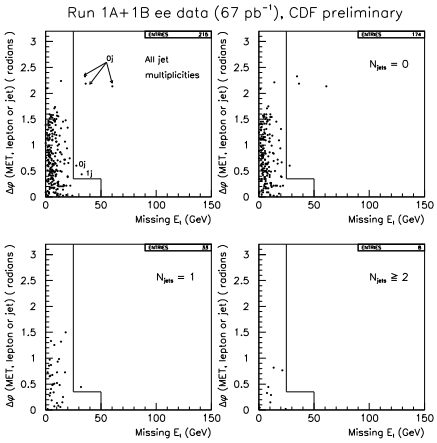

Figure 5: Scatter plot for dielectron events of Missing E_T versus $\Delta\phi$ where ϕ is the smallest angle in the transverse plane between the Missing E_T and either an electron or a jet. 0 dielectron candidates are observed.

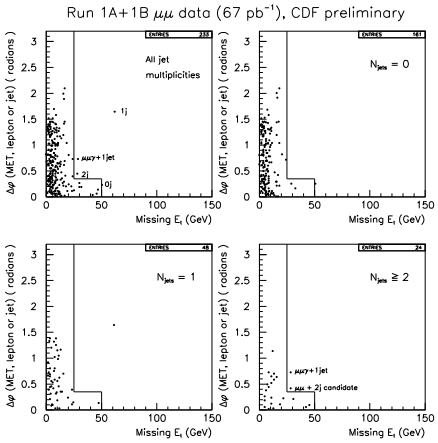

Figure 6: Scatter plot for dimuon events of Missing E_T versus $\Delta\phi$ where ϕ is the smallest angle in the transverse plane between the Missing E_T and either a muon or a jet. 2 dimuon candidates are observed. One event could be a $Z \rightarrow \mu\mu\gamma$ ($M_{\mu\mu\gamma} = 86\,GeV$). This event is removed from the sample when calculating a top signal significance. The remaining $\mu\mu$ event has an SLT tag.

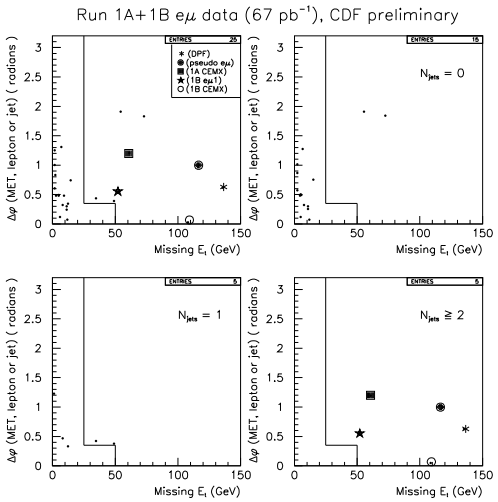

Figure 7: Scatter plot for electron-muon events of Missing E_T versus $\Delta\phi$ where ϕ is the smallest angle in the transverse plane between the Missing E_T and either a lepton or a jet. 5 $e\mu$ candidates are observed. Two are SVX-SLT double tagged.

Figure 8: Event Display for one of the e μ events. Three views are shown (Tracking, LEGO, and Vertex). The LEGO plot shows the observed calorimeter E_T in the $\eta-\phi$ plane. Tracking and Vertex views show the reconstructed tracks in the r-ϕ plane with increasing resolution.

In summary, 6 dilepton events are observed. The expected background is 1.3 ± 0.3 events. The probability of the background to fluctuate up to the signal for the dilepton events is 2.7σ. Three of the events contain a total of 5 btags, compared with an expectation of 0.5 if the events are from background. We expect 3.6 tags if the events are from $t\bar{t}$.

3. Detector

The CDF detector currently consists of a 1.4 Tesla superconducting solenoid with tracking detectors inside it. Calorimeters (electromagnetic and hadronic) are located outside the magnet and in the forward region. Muon detection is provided by chambers located outside the calorimeters in the central region. A silicon vertex detector located just outside the beam pipe is used for secondary vertex identifica-

tion. [7] Fig. 9 shows the current detector and the planned new detector for run 2.

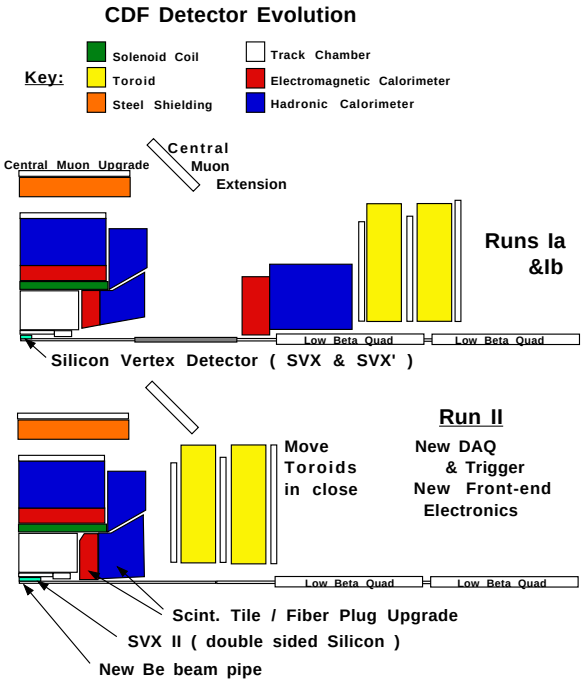

Figure 9: A cross section of the CDF detector for the current run (1995) run 1b(top) and the anticipated run 2(bottom).

For run 1b a new ac-coupled, four-layer silicon vertex detector with radiation-hard electronics, was installed. This detector is 51 cm long and has top b-tag efficiency of 42%. For run 2 we will have a new 96 cm long silicon vertex detector with an efficiency of about 80%. This detector will provide coverage in both the r-ϕ and r-z views. Detailed information about the CDF upgrade plans is found in reference. [8]

In addition to the SVX upgrade the present gas calorimeters will be replaced with new scintillator based calorimeter. Green wavelength shifting fibers will be inserted into scintillating tiles. This upgrade increases the radiation hardness of these detectors so that they will operate at a luminosity of 10^{32} cm^{-2} s^{-1}. The new electromagnetic calorimeter will contain an embedded position detector at shower maximum to improve electron identification and π/γ separation. As seen in the figure the new detector is more compact.

A scintillating fiber tracker will be added between the SVX and the CTC (Central Tracking Chamber). This device will increase the region in which we can reconstruct tracks (rapidity coverage will increase from $|\eta| < 1.4$ to 2.0).

The new running conditions will require many changes. The shorter bunch

spacings for run 2 (395 ns or even 132 ns) will require many upgrades in electronics. The increase in luminosity to 2×10^{32} cm^{-2} s^{-1} raises many interesting question relating to occupancy in the CTC. Many improvements will be needed to both the data acquisition and offline computing before we are able to process data under run 2 conditions.

4. Silicon Vertex Detector b-Physics

Much effort has been devoted to understanding and simulating the SVX detector. [9] Our understanding includes the primary ionization ($\frac{dE}{dx}$ of the ionizing particle forming electron hole pairs) the secondary ionization (δ ray) and noise. Good agreement is obtained between an inclusive electron sample (95% $b\bar{b}$) and a $b\bar{b}$ Monte Carlo. The ratio of data to Monte Carlo efficiencies is 0.96 ± 0.07.

Perhaps the best evidence that we can use the SVX detector to identify b's in the decay of the top is that we have now done many analyses on b-physics. [10] Indeed this information is now available on WWW (World Wide Web) essentially on the day it is approved. The b-Physics group has been especially active in this effort. You will have no trouble in going from the "Fermilab Home page" (Fig. 10)

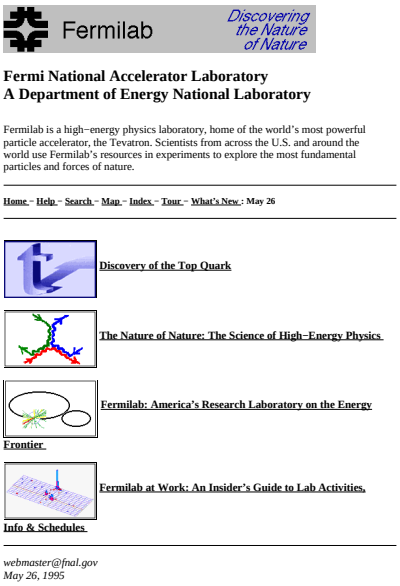

Figure 10: This is the Fermilab home page on World Wide Web (WWW).

to "Fermilab at Work" and from there to the "CDF Experiment", and from there to "CDF Physics Results" and then "Bottom". I will show two plots from this area to give a flavor of the type of data we presently have. These plots are from "B+ and B0 Lifetimes Using Exclusive B->J/psi K decays". The first plots shows the J/ψ mass peak obtained by reconstructing charged tracks (from muons) in the SVX detector (Fig. 11). The data sample of about 140 K events corresponds to an

integrated luminosity of 68 pb^{-1}. Note the mass is reconstructed with a sigma of 16 MeV. The second plot shows the reconstructed charged B mass (Fig. 12). The

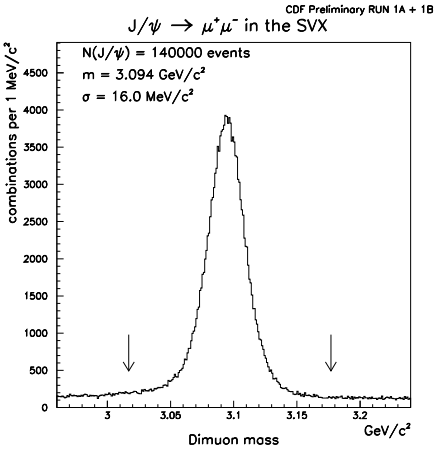

Figure 11: Invariant mass distribution of two oppositely charged muons

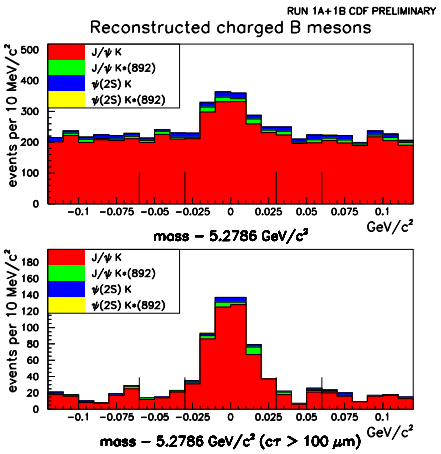

Figure 12: Reconstructed charge B mass.

charged B mass distribution is much cleaner if one requires $c\tau > 100\mu$m.

5. SVX Analysis

A simplified illustration of an event containing a b hadron with large P_T is shown in Fig. 13. The primary vertex for each event is found by a weighted fit of the SVX tracks (r,ϕ) and the VerTeX drift chamber (VTX) z vertex position. Tracks with large impact parameters are removed from the fit. The impact parameter, d, is the distance of closest approach of a track to the primary vertex in the r-ϕ plane. L_{xy} is the two dimensional decay distance to the secondary vertex from the primary vertex in the r-ϕ plane. For a top mass of about 180 GeV/c^2, the mean transverse displacement of the b decay vertex is 3 mm. The SVX tracking algorithm makes a first pass to search for 3 track vertices, and if none are found, a second pass looks for two track vertices. The error in L_{xy} is typically 130 μm ($\sigma_{L_{xy}}$). The secondary vertex is required to have a significance $L_{xy}/\sigma_{L_{xy}} > 3$. The efficiency for tagging at least one b quark in a $t\bar{t}$ event with 3 or more jets is determined from Monte Carlo simulations to be $42 \pm 5\%$. This is a considerable improvement over the SVX b-tagging for run 1a ($22 \pm 6\%$).

The reasons for the improvement are an improved SVX (ac-coupled detectors and radiation hardened electronics), an improved vertex finding algorithm, and fixing a previous bug in the Monte Carlo simulation, and better statistics in the Monte Carlo and also in the data used to check the Monte Carlo.

Fig. 14 shows as circles the number of W + n jet events before tagging. There

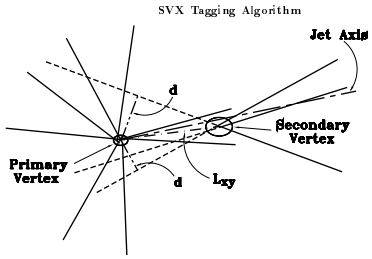

- Algorithm makes a first pass to search for 3 track vertices and then a second pass to look for 2 track vertices.
- $L_{xy}/\sigma_{L_{xy}} > 3.0$

Efficiency for tagging a $t\bar{t}$ event: 42 ± 5 %
Comparison to Run 1A

- Improved Algorithm: Factor 1.25
- Bug Fix in B baryon Lifetime: Factor 1.15
- Statistically more accurate measure of the data/MC scale factor (agree to 1-1.4 σ).

Figure 13: Simplified view of an event containing a secondary vertex. The solid lines represent charged-particle tracks reconstructed in the SVX. The primary vertex is where the $p\bar{p}$ interaction occurs. L_{xy} is the two-dimensional decay distance to the secondary vertex.

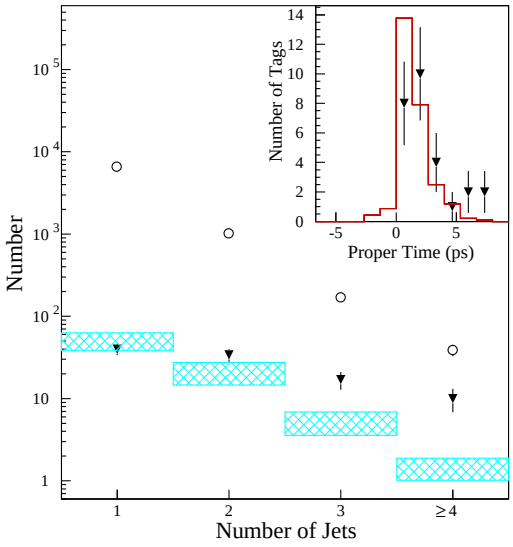

Figure 14: Number of events before SVX tagging (circles), number of tags observed(triangles) and expected number of background tags (hatched) versus jet multiplicity. The inset shows the secondary vertex proper time distribution for the 27 tagged jets in W + n $\geq$ 3 jet data (triangles) compared to the expectation for b quark jets from $t\bar{t}$ decay.

are 203 W + n $\geq$ 3 jet events. The number of W + n jet events with SVX tags are shown as triangles. The estimated background is shown as a hatched region. There are 27 SVX tags for W + n $\geq$ 3 jets. The background is calculated to be 6.7 $\pm$ 2.1 for W + n $\geq$ 3 jets. The insert shows the secondary vertex proper time distribution for the 27 tags. The solid curve shows the expected proper time distribution for b quark jets from a $t\bar{t}$ Monte Carlo. Clearly the distribution agrees with expectations.

We have a very large sample of W + n jet events before tagging. These events have been compared with the VECBOS Monte Carlo. [11] Fig. 15 is taken from a W sample of 48 K events (integrated luminosity of 73 pb^{-1}). The plots shows the E_T

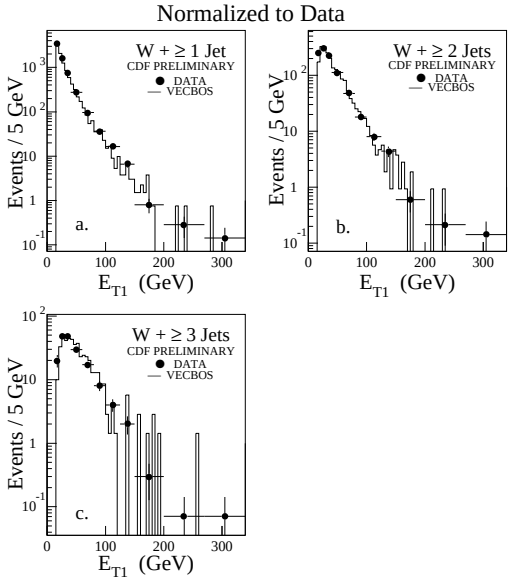

Figure 15: Comparisons between CDF data and VECBOS for W + JETS.

spectra for events with one or more jets, two or more jets and three or more jets. The VECBOS Monte Carlo is run with Q^2 scale equal to the square of the average P_T of the jets. Good agreement is obtained. This good agreement is nice but not so crucial in understanding top backgrounds, as described below.

The largest background for SVX tagging is caused by a gluon jet in a W event splitting into a heavy flavor pair. The second largest background is due to "Mistags" where a light quark jet in a W event is tagged as a b jet due to resolution smearing or errors. Other backgrounds such as flavor excitation (sg $\rightarrow$ Wc), WW, WZ, Z$\rightarrow$ $\tau\tau$ and non-W $b\bar{b}$ are also significant (Table. 3).

The most reliable method is to use Monte Carlo simulations for all processes except for the "Mistags". The "Mistags" are estimated using the negative decay length tags observed in di-jet samples. The sum of all the backgrounds is 6.7 $\pm$ 2.1 tags.

Fig. 16 shows a tagged lepton plus jet event. In this case both b-jets are tagged

Figure 16: Event Display for an SVX b-tagged event. Tracking, LEGO and Vertex views are shown.

by the SVX. The lowest chi-squared assignment (see the section on Mass Analysis) corresponds to the assignments $t \rightarrow W^+ b$(jet 4), where the $W^+ \rightarrow e^+ + \nu$ and the $\bar{t} \rightarrow W^- \bar{b}$, where the W^- goes to jet(2) and jet(3), and jet(1) corresponds to $\bar{b}$.

6. Cross Section

In this section we give the results for the number of events obtained in the dilepton, SVX and SLT channels. The results are presented for both run 1a and the present sample from run 1a + 1b ($67 pb^{-1}$). Our present result for the probability of the background to reproduce the signal is 4.8σ. This result is based on 6 dilepton events and 37 b-tagged events. The relevant numbers are 6 dilepton events with a background of 1.3 ± 0.3 events, 27 SVX tags (in 21 events) with a background of 6.7 ± 2.1 tags and 23 SLT tags (in 22 events) with a background of 15.4 ± 2.0 tags.

Fig. 17 gives a new preliminary value for the $t\bar{t}$ production cross section of $7.6^{+2.4}_{-2.0}$ pb. This number is based on all three measurements (dilepton, SVX, SLT).

⋆ **Cross Section (Preliminary)**
$\sigma = 7.6\ ^{+2.4}_{-2.0}$ pb

Dilepton Channel
Lepton Plus Jets Channel
SVX Silicon vertex b-tagging
SLT Soft Lepton b-tagging

- Run 1a + 1b Luminosity = $67 \pm 4.85\ pb^{-1}$

DL 7 events Background 1.3 ± 0.3
$\epsilon = 0.78 \pm 0.08\ \%$
$\sigma = 10.9\ ^{+5.9}_{-4.5}$ pb
SVX 21 events Corrected-Background 5.5 ± 1.8
$\epsilon = 3.38 \pm 0.87\ \%$
$\sigma = 6.8\ ^{+2.9}_{-2.3}$ pb
SLT 22 events Corrected-Background 14.7 ± 2.2
$\epsilon = 1.73 \pm 0.29\ \%$
$\sigma = 6.3\ ^{+5.0}_{-4.1}$ pb

Figure 17: The cross section (preliminary) from run 1a + 1b from 67 pb^{-1} using dilepton, SVX and SLT data.

Our "total efficiency × acceptance " for the SVX of 3.38% is the product of the branching ratio (29.6%), the lepton plus jets selection efficiency of 8.1% and the SVX tagging efficiency of 42%. Similarly the SLT "total efficiency × acceptance" of 1.73% is the product of the branching ratio (29.6%), the lepton plus jets selection efficiency of 8.1% and the SLT tagging efficiency of 22%.

The cross section is compared to the theory [12] (next-to-next-to leading order) in Fig. 18. The new value is a little higher than the theory value but is consistent

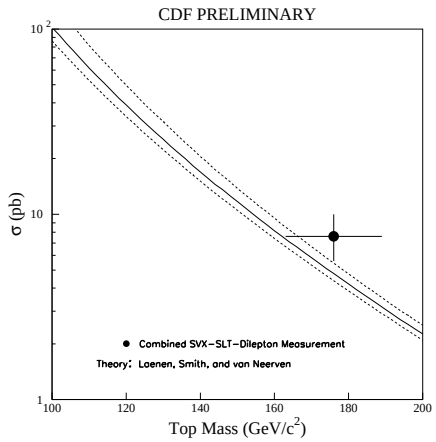

$$\sigma(t\bar{t}) = 7.6\ ^{+2.4}_{-2.0}\ pb$$

Figure 18: The preliminary CDF data point and a theory curve from Laenen *et al*.

with it within the errors.

7. Mass Analysis

The process

$$p\bar{p} \rightarrow t\bar{t} + X$$

as displayed in Fig. 19 is kinematically constrained. In this five vertex system we have assumed that the initial $p\bar{p}$ system has a net momentum of zero and an energy of 1.8 TeV. We further assume the mass of t and $\bar{t}$ are the same. Further details of the fitting method are given in reference 13. From the measured jet energies we must correct for missing energy (μ's or neutrinos) as well as for energy that is outside the jet cone we are using (ΔR = 0.4). Reference [13] contains further information on jet corrections. The system of equations yields an overconstrained system of 20 equations in 18 unknowns (2C-fit). As we do not measure the longitudinal component of the energy, there are two possible solutions for the P_Z of the neutrino. There are 24 possible combinations because you select b_1 from the 4 jets, then you select b_2 from the remaining 3 jets, and you have two choices for the P_Z of the neutrino. In most cases these two solutions are almost identical with regard to the mass of the top quark. Of the 24 different combinations the one with the lowest χ^2 is selected. If a b is tagged the number of solutions is only 12 and if two b's are tagged the number of solutions is only 4.

The final pretagged sample (with no b tagging) used in the mass analysis contains 88 events. The top mass has been computed by three independent groups within CDF using slightly different methods. The results using the MINUIT fitter are presented here. Much the same mass is obtained when the top background

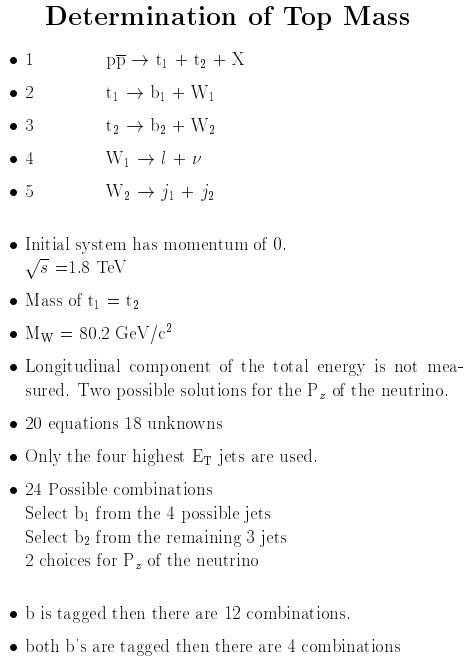

Figure 19: An overview of the mass fitting.

is constrained (176.1 $\pm$ 8.6 GeV/c^2) and when it is not (174.6 $\pm$ 7.7 GeV/c^2). The shape of the fitted background is obtained from the VECBOS Monte Carlo. The reconstructed mass spectrum is given in Fig. 20. The figure also shows the constrained background fit. It is clear that there is a signal of top events. The distribution is consistent with the predicted mix of approximately 30% $t\bar{t}$ and 70% W + jet background (VECBOS).

The situation is even clearer when we use the b-tagged sample. The final sample with b tagging used in the mass analysis contains 19 events. This b-tagged sample uses both the SVX and SLT tags. The mass obtained from the MINUIT fitter is 175.6 $\pm$ 7.8 GeV/c^2 for the constrained fit and 175.0 $\pm$ 6.7 GeV/c^2 for the unconstrained fit. The reconstructed mass spectrum is given in Fig. 21.

The systematic errors are given in table 4. The largest error is the absolute jet energy scale. The accuracy is determined from photon-jet and Z-jet balancing.

Our top mass measurement can be combined with our recent measurement from run 1a of the W mass. The results are presented in Fig. 22. We see that almost no limitations are placed on the Higgs mass. The situation will improve considerably when run 2 is complete. Run 2 is expected to have an integrated luminosity of more than 1000 pb^{-1} (best estimate is 2000pb^{-1}). For an integrated luminosity of 1000pb^{-1} the estimated uncertainty in the W mass is expected to be 45 MeV/c^2 and the uncertainty in the top mass is expected to be 4 GeV/c^2.

I will present additional information on the CDF top analysis in the next paper

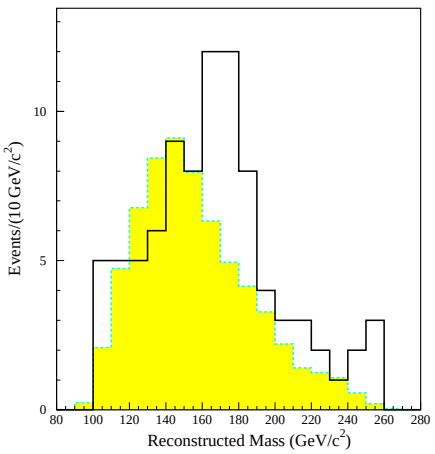

Figure 20: The reconstructed mass of the pretagged sample. The background is constrained to 65 events.

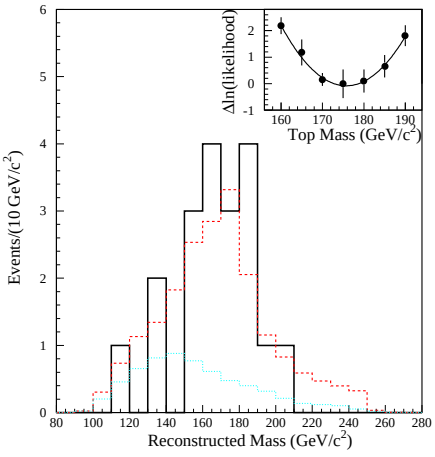

Figure 21: The reconstructed mass of the tagged sample. Also shown are the background shape (dotted) and the sum of background plus $t\bar{t}$ Monte Carlo simulations for M_{top} = 175 GeV/c^2 (dashed), with the background constrained to the calculated value of $6.9^{+2.5}_{-1.9}$ events. The inset shows the likelihood fit used to determine the top mass.

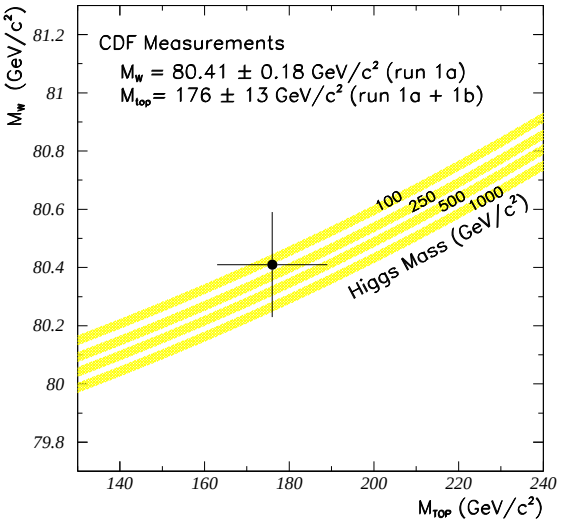

Figure 22: M_W versus M_{TOP} as measured by CDF (May, 1995). For run 2 we estimate the uncertainty in the top mass will be 4 GeV and the uncertainty in the W mass will be 45 MeV.

Table 4. Systematic uncertainties in top mass measurement, obtained from Monte Carlo or data.

Systematics	(GeV)	(%)
a. Absolute Jet Energy Scale (detector effects)	3.1	1.8
b. Relative (Plug-Central) Energy Scale	0.1	<0.1
c. Absolute Energy Scale (Gluon Effects)	7.7	4.4
d. Fit Configuration	2.5	1.4
e. Signal shift due to SLT tag	2.1	1.2
f. Signal shift due to SVX tag	1.1	0.6
g. Background shift due to SLT mistag	0.1	<0.1
h. Background shift due to SVX mistag	0.1	<0.1
i. Different background shapes	1.6	0.9
j. Different type of likelihood fit	1.6	0.9
k. Different way to fit the points	1.2	0.7
l. Monte Carlo statistics	3.1	1.8
Total	9.8	5.6

("Kinematics of the $t\bar{t}$ events in W + Jets at CDF"). I will show the reconstructed mass of the $t\bar{t}$ system for a b tagged sample of 19 events.

Acknowledgements

I would like to thank the organizers of this conference for their hospitality. I would also like to thank my collaborators for help with this paper, especially G. Bellettini, M. Binkley, J. Skarha, and G.P. Yeh. Thanks also go to R. Herber for help with PostScript.

References

1. F. Abe *et al.*, Phys. Rev. Lett. **74**, 2626 (1995).
2. F. Abe *et al.*, Phys. Rev. Lett. **64**, 142 (1990).
   F. Abe *et al.*, Phys. Rev. D **43**, 664 (1991).
   F. Abe *et al.*, Phys. Rev. Lett. **64**, 147 (1990).
   F. Abe *et al.*, Phys. Rev. Lett. **68**, 447 (1992).
   F. Abe *et al.*, Phys. Rev. D **45**, 3921 (1992).
3. F. Abe *et al.*, Phys. Rev. Lett. **73**, 225 (1994).
   F. Abe *et al.*, Phys. Rev. D **50**, 2966 (1994).
4. F. Abe *et al.*, Phys. Rev. D **51**, 4623 (1995).
5. V. Bharadwaj, "Status and Future of the Tevatron" 10th Topical Workshop on Proton-Antiproton Collider Physics, Fermilab May, 1995.
6. G. William Foster, "The TeV33 Project" 10th Topical Workshop on Proton-Antiproton

Collider Physics, Fermilab May,1995.
7. D. Amidei *et al.*, Nucl. Instrum. and Meth. **A350**, 73 (1994).
8. The CDF Upgrade,CDF/DOC/PUBLIC/3171, submitted to the Fermilab Directorate June, 1995.
9. J. Incandela, "Top Decay to Lepton + Jets: CDF B Tags and Cross Section" 10th Topical Workshop on Proton-Antiproton Collider Physics, Fermilab May 1995.
10. F. Abe *et al.*, Phys. Rev. Lett. **71**, 1685 (1993).
    F. Abe *et al.*, Phys. Rev. Lett. **71**, 3421 (1993).
    F. Abe *et al.*, Phys. Rev. Lett. **72**, 3457 (1994).
    F. Abe *et al.*, Phys. Rev. Lett. **74**, 4988 (1995).
11. F.A. Berends, W.T. Giele, H. Kuijf, and B. Tausk, Nucl. Phys. **B357**, 32, (1991).
12. E. Laenen, J. Smith, and W.L. van Neerven, Phys. Lett. **B321**, 254 (1994).
13. Steve Vejcik, "Measurement of the Top Quark Mass at CDF" 10th Topical Workshop on Proton-Antiproton Collider Physics, Fermilab May, 1995.